Structure of Polyethylene After Pulse Ion Beam Treatment

NIKOLAY GAVRILOV,[1] **DINA YAKUSHEVA,**[2] **ALEXEY KONDYURIN**[2]

[1]Institute of Electrophysics, Russian Academy of Science, 34 Komsomolskaya St., Ekaterinburg, Russia

[2]Institute of Technical Chemistry, Russian Academy of Science, 13 Lenin st., Perm 614000, Russia

Received 1 March 1996; accepted 29 December 1997

ABSTRACT: Pulse ion beam treatment was employed for polyethylene (PE) surface modification. Ultraviolet, infrared (IR), IR–attenuated total reflection spectroscopy (IR–ATR), and X-ray photoelectron spectroscopy methods, as well as wetting angle measurement, were used for the analysis of PE structural changes. Theoretical calculations and experimental data showed treated PE surfaces to have a layered structure. It was found that the upper layer contains various products of PE oxidation and the lower layer contains products of PE decomposition, that is, condensed aromatic structures. © 1998 John Wiley & Sons, Inc. J Appl Polym Sci 69: 1071–1077, 1998

Key words: ion beam treatment; polyethylene; surface; spectroscopy

INTRODUCTION

Recently, modification of polymer materials (PM) by ion beam surface treatment (IBEST) draws increasing attention of researchers. IBEST induces structural changes in the surface layer of polymer film, the depth of the modified layer, and the degree of modification, being dependent on treatment conditions;[1,2] for example, in Schnabel and Klaumunzer,[3] the number of crosslinks is supposed to be dependent on linear energy transformation (LET), ion energy, and irradiation dose. Thus, IBEST of PM leads to an abrupt change of thin film physical properties or modifies the surface layer of the polymer material sample.[3–5]

It was shown that many operating characteristics of polymer surface are modified as a result of IBEST, such as conductivity[6–13] (i.e., high conductive polymer layers are obtained), optical properties,[10–12,14,15] adhesion,[16] and wear resistance.[17,18]

According to current knowledge, high energy ions of the beam scatter on the target atoms, and dissipating energy always causes some changes in polymer macromolecule structure. The dominating mechanism for energy transfer from ions to polymer is inelastic collisions, referred to as electronic stopping, which affects the energy level of the electrons.[19] Electron exitations lead to the formation of free radicals and, consequently, chemical reactions in the polymer. Polymer chain rupture, crosslinks, unsaturated bond formation, and gas liberation[12] take place as a result of ion irradiation, with relatively low doses being employed. Thus, various structures are formed, including regions of condensed aromatic structures. Depending on the treatment dose value, one or another of carbonization degree of PM is observed.[1,2,13,19–22] That is to say, the irradiated polymer contains local structures analogous to structure of polymer high-temperature degradation products.

As a rule, in order to avoid heating up of the sample, low beam current densities, 0.05–5 μA/cm^2,[5,21,23] are used for modification of PM. However, the use of higher current densities is a matter of interest for researchers. A pulse periodical regime allows an increase of the current density

---

Correspondence to: A. Kondyurin.

Contract grant sponsors: Sandia Laboratories (S.L.) and the Russian Academy of Science; contract grant number: AM-2869 (from S.L.).

Journal of Applied Polymer Science, Vol. 69, 1071–1077 (1998)
CCC 0021-8995/98/061071-07

in the beam, without a risk of thermal decomposition of PM. The use of the beam with high current density allows the same degree of modification to be achieved in a minimal period of time. Besides, the formation of some structures different from those after treatment at low current densities is possible. Pulse current density can be increased by several orders, while average current density remains unaffected.

The wide range of polymers, affected by ion beams at various regimes of IBEST, such as aliphatic (polyethylene[22,23] and polypropylene[4,5,23]), aromatic (polystyrene[3,21,22]), and some others,[3,23–25] have been studied already. Polyethylene (PE) was chosen as one of the subjects of inquiry, as its relatively simple structure allows more conclusive interpretation of experimental data to be carried out. The reasons for this choice are its availability and low price and, in consequence, the prospect of wide practical application of modified PE.

In this work, pulse periodical regimes were used for treatment of low-density PE by a nitrogen ion beam.

EXPERIMENT

Industrial low-density PE as 50-μm-thick film without fillers and plasticizers was employed for treatment. PE contained antioxidant *N*-phenylnaphtylamine-1. PE film was implanted by the ion source “Pulsar” (Institute of Electrophysics, Ekaterinburg, Russia), utilizing the pulse nitrogen ion beam with an ion energy of 30 and 20 keV, a current density of 5 mA/cm^2, pulse duration of 1 and 0.3 ms, and pulse frequency of 1 and 3 Hz.

Wetting angle was measured with an MBR-10 microscope according to geometrical sizes of drops of wetting liquids. Wetting angle was determined for the following 4 liquids: water, glycerine, formamide, and ethylene glycol. Surface energy was calculated by the regression method from the following equation:[26]

$$\frac{\sigma_2(1 + \cos\theta)}{\sqrt{\sigma_2}} = \sqrt{\sigma_1^d} + \sqrt{\sigma_1^p}\,\frac{\sqrt{\sigma_2^p}}{\sqrt{\sigma_2^d}}$$

where σ_1 and σ_2 are the polymer surface energy and the wetting liquid energy, respectively, and θ is the wetting angle. Infrared attenuated total reflection (IR ATR) spectra were recorded using a UR-20 spectrometer and a Specord M-82 (Carl Zeiss Jena, Germany) and Fourier Bomem spectrometer with an ATR accessory, containing a KRS-5 crystal (the angle of reflection is 45° and the number of reflection is 25). UV transmission and reflection spectra were recorded using a Specord M-40 spectrometer with a reflection accessory at an angle of 8°. X-ray photoelectron spectra (XPS) were recorded using a magnetic spectrometer (Physical and Technical Institute, Izhevsk, Russia).[27]

RESULTS

It was necessary at the initial stage of the work to confirm that use of the pulse regime of treatment does not cause melting and destruction of PM. The steady-state temperature of the sample (PE film) was 323 K at a pulse frequency of 2 Hz, a pulse current density equal to 5 mA/cm^2, and a treatment dose of 10^{16} ion/cm^2. Consequently, macroheating up does not occur. Average current density at such regime constitutes 10 mA/cm^2.

Further, the frequency of pulse repetition of 1 Hz was used, and the average current density doesn’t exceed 5 mA/cm^2. No change of 1896 and 2020 cm^{-1} band intensity in polarization IR transmission spectra at various light polarization has been observed. This confirms the orientation of macromolecules in PE film to be unchanged. The process of microheating up (i.e., local processes of melting, recrystallization, and thermal degradation) does not occur.

No change in the ratio of crystal and amorphous phases bands intensities in IR ATR spectra in the area of doublet 720, 730 cm^{-1} has been observed, evidence that the surface layer of PE film was not overheated and recrystallized too.

The change of PE surface wetting angle with different liquids has been observed at relatively low treatment doses (Fig. 1). The wetting angle of PE with water and formamide decreases as the treatment dose increases. However, wetting angle values do not reach those for temperature-treated (45°) and plasma-treated (10^0) PE. The glycerine and ethylene glycole wetting angle was practically unaffected. The change of the wetting angle is caused by the change of intermolecular interaction between PE surface layer molecules and wetting liquid. No changes in wetting angles of treated PE were observed during a year after IBEST.

As is known, the total surface energy, as well as its polar and dispersion parts, can be calculated from the wetting angle data. Results of surface

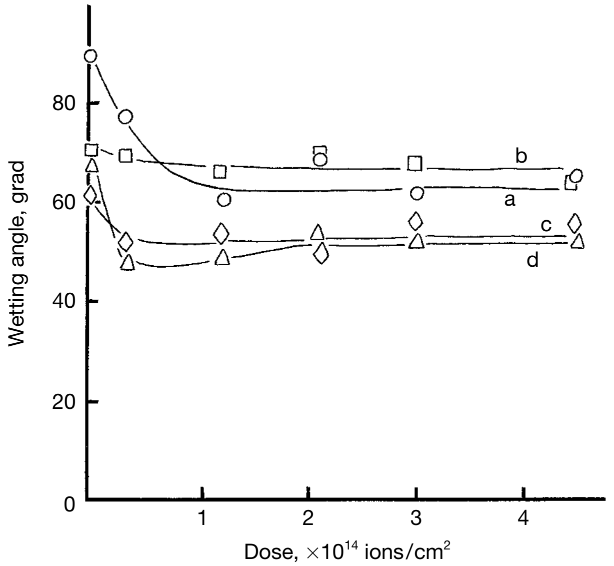

Figure 1 Wetting angle of (a) water, (b) glycerine, (c) ethyleneglycole, and (d) formamide on PE surface treated at different doses.

energy calculation for treated and untreated PE samples on the basis of wetting angle measurements for four liquids are summarized in Table I. Some increase of the total surface energy with the increase of treatment dose has been observed. The contributions of the polar and disperse components of the total surface energy change more significantly as a result of the polar component increase and the nonpolar component decrease.

In XPS spectra of PE after IBEST, an asymmetric peak related to C1s is observed (Fig. 2). Its shoulder is formed by bands with energies of 286.2, 287.0, and 288.2 eV. These bands are correlated to carbon, taking part in —C—O—, —C=O and —O—C=O groups, respectively. No bands of carbon participating in condensed aromatic structures at 284.6 eV[28] have been found. Oxygen lines of O1s with the energies of 531.3 and 535.8 eV related to oxygen, present in —C—O— and —C=O groups, have been observed. One can notice that the intensities of O1s and C1s bands of oxygen-containing groups are of the same order of magnitude, and that the intensity of the C1s band correlated to carbon of polyethylene chain. No N1s bands in XPS spectrum have been observed.

Owing to the fact that XPS (with CuK$_\alpha$ band) analyses about a 100 Å thick surface layer of PE film, one can conclude that after IBEST significant oxidation takes place in the 100-Å-thick surface layer, whereas carbonization does not take place at this depth.

In UV reflection spectra of PE film after IBEST, no bands related to unsaturated carbon–carbon bonds have been detected (Fig. 3). In contradiction to the initial PE spectrum, in the PE spectrum after IBEST, absorbtion bands at 217 and 231 nm, related to carbonyl absorption, emerge. The intensity of this bands grows linearly with treatment dose increase (Fig. 4). UV reflection spectra of PE allows an analysis of the 200–500-Å thick surface layer across the wave band to be carried out. Consequently, at a given depth, no carbonized layers have been detected. Exclusively oxidation of treated PE has been observed.

Emergence of wide overlapping bands in the area of 1600–1750 cm^{-1} in IR ATR spectrum of PE surface after IBEST can be related to valency vibrations ν(C=C) of polyenic and condensed aromatic structures (Fig. 5). As the extinction coefficient of these bands is small,[29] it can be stated that concentration of unsaturated groups is rather high. When treatment dose increases, the unsaturated group concentration grows linearly. In the IR ATR spectra of treated PE, the appearance of bands at out-of-plane modes γ(=CH—) region at 968.2 and 907.9 cm^{-1} has been observed. The first band can be related to the corresponding mode of transvinilene group, whereas the second one can be related to the mode of vinyl group. Intensity of 881.1 cm^{-1} line corresponding to end vinylidene groups decreases somewhat. Intensity of 968.2 and 907.9 cm^{-1} lines is very low and can be compared to the intensities of the lines, corresponding to unsaturated groups. No lines in the area of the stretching modes of C—H bond of unsaturated groups have been detected at the region of 3000–3100 cm^{-1}. Having compared the intensities of the lines, related to unsaturated carbon–carbon bonds, one may draw the following conclusion: in the surface layer of PE after IBEST, the concentration of hydrogen (involved in unsatu-

Table I Surface Energy of PE after IBEST N$^+$

Dose (10^{14} ion/cm^2)	Surface Energy (MJ/m)		
	Full	Polar	Dispersic
0	26.2	6.4	19.8
1.2	39.7	29.8	10.0
2.1	37.9	31.3	6.2
3.0	38.9	29.9	9.2
4.5	37.4	24.9	12.4

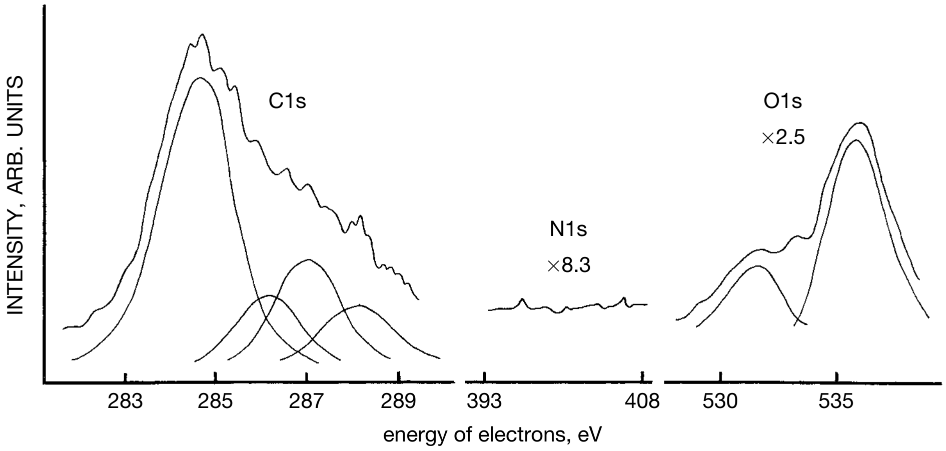

Figure 2 XPS spectra of ion beam treated PE at 10^{16} ion/cm^2 dose. Intensity of N1s and O1s regions are increased to 8.3 and 2.5 times.

rated bond) at sp^2-hybridized carbon atom is small if compared with its stoichiometric concentration in conjugated polyenic structures. Therefore, one may speak about formation of the condensed aromatic structures.

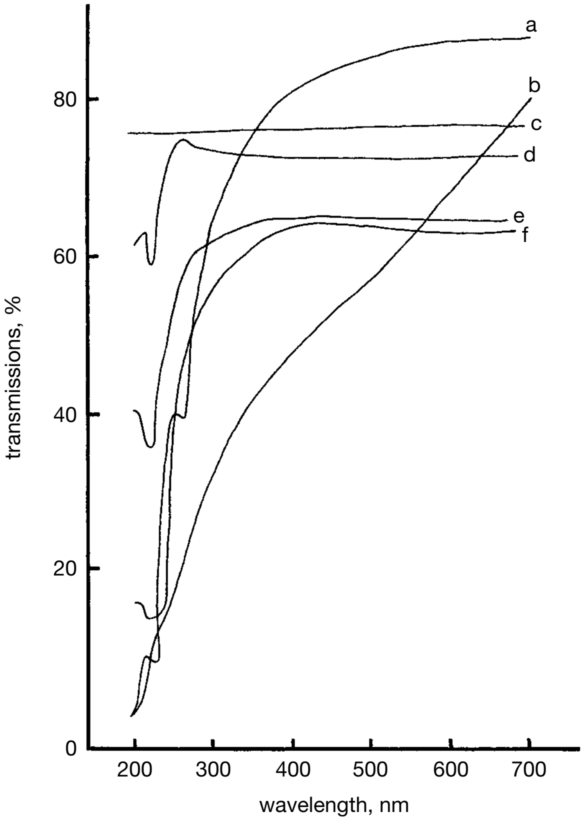

Figure 3 UV spectra of PE: (a) initial, transmission; (b) 6 × 10^{14} ion/cm^2, transmission; (c) initial, reflection; (d) 0.6 × 10^{14} ion/cm^2, reflection; (f) 1.2 × 10^{14} ion/cm^2, reflection; (g) 2.1 × 10^{14} ion/cm^2, reflection.

In IR ATR spectra of PE after IBEST, the lines appearing at the region of 1680–1750 cm^{-1} should be related to carbonyl group vibrations. Overlapping of a number of bands has been observed there as well. Having used the method of contour division[30] and carried out lines relation according data in the literature,[29] one may distinguish the following bands: 1726.5 cm^{-1}, kethone; 1740.5 cm^{-1}, aldehide; 1754 cm^{-1}, ester; 1708 cm^{-1}, carboxyl; 1706 and 1718 cm^{-1}, carbonyl in carbonized area. Oxygen-containing group concentration estimated by optical density of corresponding bands is growing linearly with the increase of treatment dose (Fig. 5). No other bands relating to oxygen-containing groups have been detected. No changes

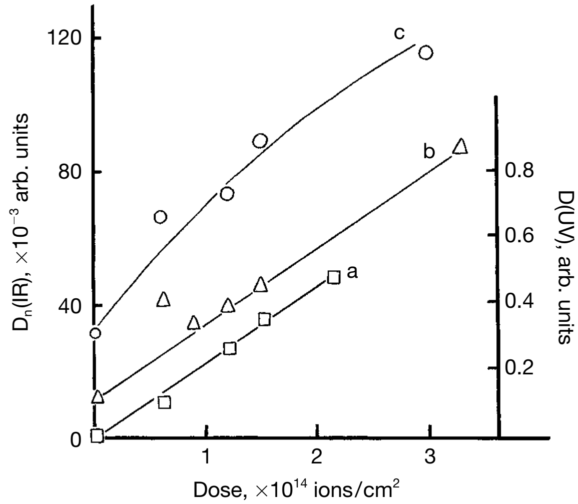

Figure 4 Intensity of PE spectral bands: (a) UV reflection, 217 nm band; (b) IR ATR, ν(C=C) = 1610 cm^{-1}; (c) IR ATR, ν(C=O) = 1720 cm^{-1}.

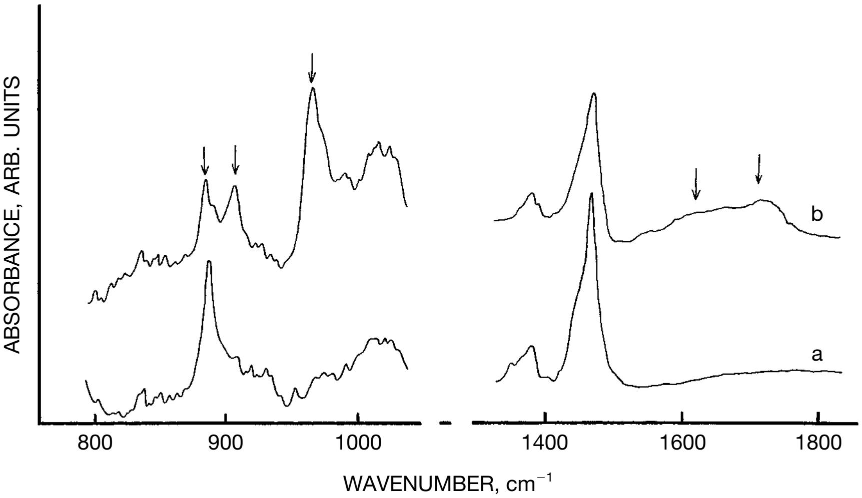

Figure 5 IR ATR spectra of (a) initial and (b) ion beam treated at 3×10^{14} ion/cm^2 dose PE. Intensity of 800–1000 cm^{-1} region is increased to 30 times.

in IR ATR spectra of treated PE were observed during a year after IBEST.

In UV-transmission spectra of PE film after IBEST, a low-frequency shoulder has been observed (Fig. 3). One can connect its emergence with the absorption of condensed aromatic structures of the carbonized layer. The treatment dose increase leads to the conjugation number increase and an absorption band shift to the long wavelength spectrum area. At 10^{15} ion/cm^2 treatment dose, a 550 nm absorption boundary has been observed. According to the UV spectra empirical relationship,[31] this corresponds to the formation of condensed aromatic system, containing 5 rings.

DISCUSSION

The process of ion implantation was simulated on computer with the aid of the calculation program TRIM 91.[32,33] The calculated density of H atom vacancies in treated PE as a function of depth is shown in Figure 6. A similar dependence is observed for C atom vacancies. Formation of C and H atom vacancies leads to free radical reactions in treated PE. So, the distribution of macromolecule structure defects corresponds to the distribution of ion-beam-induced defects.

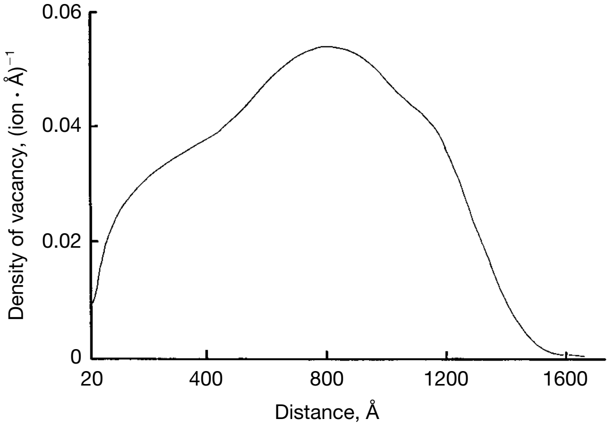

Figure 6 Vacancy concentration of recoiled H atoms of PE treated by N$^+$ (20 keV).

According to calculation results, the upper layer is only slightly modified. In this layer, the ion with high energy and pulse knocks the hydrogen and carbon atoms out, and the direction of their movement does not change significantly. The gradual increase of defect number with the increase of penetration depth has been observed. The symbolic boundary of this layer is located at the distance of 500 Å from the polymer surface. Then ion loses its energy so that its collisions with polymer atoms can result in the change of its trajectory and trajectory of recoiled atoms. This layer is characterized by a high structure defect concentration and a high value of energy transfer from ion to target atoms. The sum of ion and knocked atoms energy losses reaches 22 eV/Å. At such LET values, significant modification of the PE structure should be observed.[34] Thus, the surface area of treated PE may be considered as consisting from two layers with different composition and structure.

Experimental data verify the complex structure of the PE surface layer after IBEST. Methods of wetting angle measurement, XPS, and UV reflection spectroscopy proved that treated PE macromolecules include oxygen-containing groups. It has been detected that no carbonization or unsaturated carbon–carbon bonds are formed. Besides the small defects concentration, this layer is characterized by high oxygen content, caused by diffusion of the oxygen atoms to the bulk of the sample, produced from the ion gun chamber.

Destruction of the deeper (the distance of 500–1000 Å from the surface) layer is more intensive, with condensed aromatic structures being formed. The thickness of this layer is small, so one may observe the bands of deeper undestructed PE layers (to 5000 Å) in IR ATR spectra.

Analysis of experimental data showed that continuous IBEST at low current densities and pulse periodic IBEST at high current densities exert a similar effect on polymer sample. That is, the pulse periodical IBEST regime allows one to obtain surface layers with structure and properties analogous to that of polymer after continuous IBEST. The current density increase at pulse periodical IBEST leads to a treatment time decrease, with other conditions being equal.

CONCLUSION

Pulse periodical IBEST causes significant changes in the structure of PE surface layer. According to theoretical simulation for low current continuous IBEST and experimental studies of PE after pulse periodical, IBEST of PE surface area is nonhomogeneous as to its structure and composition and can be schematically divided into two layers. The first layer (to 500 Å depth) is characterized by an insignificant change of structure, mainly connected with the emergence of oxygen-containing groups. The second layer contains condensed aromatic structures, and, in this layer, PE structure is highly disrupted.

Consequently, pulse periodical IBEST can be used for modification of PE structure and operating characteristics side by side with continuous IBEST. The increase of current density at pulse periodic IBEST allows the shortening treatment time, making the use of the periodical regime of IBEST more preferable.

The authors thank Vladimir Smirnov for XPS spectra.

REFERENCES

1. H. Mazurek, E. W. Maby, J. S. Abel, S. D. Senturia, and M. S. Dresselhaus, *J. Polym. Sci.,* **A21,** 537 (1983).
2. T. Venkatesan, S. R. Forrest, M. L. Kaplan, P. H. Schmidt, C. A. Murray, W. L. Brown, B. J. Wikens, R. F. Roberts, L. Rupp, and H. Schonhorn, *J. Appl. Phys.,* **56,** 2778 (1984).
3. W. Schnabel and S. Klaumunzer, *Radiat. Phys. Chem.,* **37,** 131 (1991).
4. U. W. Gedde, K. Pellfolk, M. Braun, and G. Rodehed, *J. Appl. Polym. Sci.,* **39,** 477 (1990).
5. V. Svorcic, V. Rybka, K. Volka, V. Hnatowicz, J. Kvitek, and P. Seidl, *Jpn. J. Appl. Phys.,* **31,** L287 (1992).
6. T. Hioki, S. Noda, and M. Sugiura, *J. Appl. Phys. Lett.,* **43,** 30, 1983.
7. T. Venkatesan, S. R. Forrest, and M. L. Kaplan, *J. Appl. Phys.,* **54,** 3150 (1983).
8. B. Wasserman, M. S. Dresselhaus, and G. Braunstein, *J. Electron. Mater.,* **14,** 157 (1985).
9. K. Joshida and M. Iwaki, *Nucl. Instrum. Methods,* **B19/20,** 878 (1987).
10. M. Z. Kaplan, S. R. Forrest, P. H. Shmidt, and F. Venkateson, *J. Appl. Phys.,* **55,** 732 (1984).
11. T. S. Zhuravleva, A. V. Vannikov, O. L. Lazoreva, A. M. Shegolichin, G. A. Vinogradov, V. A. Ryaboshapko, and L. A. Evnuhiev, *J. Mol. Electron.,* **5,** 87 (1989).
12. J. Davenas, X. L. Xu, G. Boiteux, and D. Sage, *Nucl. Instrum. Methods,* **B39,** 754 (1989).
13. I. H. Loh, R. W. Oliver, and P. Sioshansi, *Nucl. Instr. and Meth.,* **B34,** 337 (1988).
14. B. S. Elman, M. R. Thakun, D. I. Sandman, and M. A. Newklik, *J. Appl. Phys.,* **57,** 1996 (1985).
15. J. Davenas, X. L. Xu, G. Boiteaux, and D. Sage, *Nucl. Instr. and Meth.,* **B39,** 759 (1989).
16. G. A. Mesyats, Y. S. Klyachkin, N. V. Gavrilov, V. N. Mizgulin, R. M. Yakushev, A. V. Kondyurin, *Vacuum,* **47,** 1085 (1996).
17. E. H. Lee, M. B. Lewis, B. I. Blansand, and I. K. Mansur, *J. Mater. Res.,* **6,** 610 (1991).
18. S. L. Koul, L. T. Chadderton, D. W. Fink, and S. A. Cruz, *Nucl. Tracks Radiat. Meas.,* **19,** 825 (1991).
19. G. M. Mladenov, M. Braun, B. Emmoth, and J. P. Biersack, *J. Appl. Phys.,* **58,** 2534 (1985).
20. J. Robertson, *Adv. Phys.,* **35,** 317 (1986).
21. A. J. Dann, M. R. Fahy, C. Jeynes, and M. R. Willis, *J. Phys.,* **D19,** L217 (1986).
22. L. Calcagno, G. Compagnini, and G. Foti, *Nucl. Instr. and Meth.,* **B65,** 413 (1992).
23. T. Sasuga, S. Kawanishi, M. Nishii, T. Seguchi, and I. Kohno, *Radiat. Phys. Chem.,* **37,** 135 (1991).
24. A. V. Leontyev, E. F. Ostretsov, V. V. Grigoryev, and E. F. Komarov, *Nucl. Instr. and Meth.,* **B65,** 438 (1992).
25. D. Karpuzov, K. L. Kostov, E. Venkova, P. Kirova, I. Katarjiev, and G. Karter, *Nucl. Instr. and Meth.,* **B39,** 787 (1989).
26. V. D. Babayants and S. G. Sannikov, *Kolloidn. Zh.,* **50,** 558 (1988).

27. O. M. Kanunnikova, F. Z. Gilmutdinov, V. I. Kozhevnikov, and V. A. Trapeznikov, *Methods of XPS Studies for Inorganic Materials* (in Russian), Udmurt University, Izhevsk, 1992.
28. *Practical Surface Analysis by Auger and X-ray Photoelectron Spectroscopy,* D. Briggs and M. P. Seah, Eds., John Wiley & Sons, New York, 1983.
29. J. Dechant, R. Danz, W. Kimmer, and R. Schmolke, *Ultrarot Spektroskopische Untersuchungen an Polymeren,* Akademie–Verlag, Berlin, 1972.
30. A. V. Kondyurin, *J. Appl. Polym. Sci.,* to appear.
31. M. Onozuka, M. Ashina, *J. Macromol. Sci., Rev. Macromol. Chem.,* **C3,** 235 (1969).
32. J. F. Ziegler and J. P. Biersack, *The Stopping and Range of Ions in Solids,* Pergamon, New York, 1985.
33. J. F. Ziegler and J. Manoyan, *Nucl. Instr. Meth.,* **B35,** 215 (1988).
34. R. M. Papaleo, M. A. de Aranjo, R. P. Livi, *Nucl. Instrum. Methods,* **B65,** 442 (1992).